Effect of object potentials on the wake of a flowing plasma

I. Katz, M. J. Mandell, and D. E. Parks
S-Cubed, P. O. Box 1620, La Jolla, California 92038

K. Wright
Department of Physics, University of Alabama, Huntsville, Alabama 3582

N. H. Stone
Space Science Laboratory, NASA Marshall Space Flight Center, Huntsville, Alabama 35812

U. Samir
Space Physics Research Laboratory, University of Michigan, Ann Arbor, Michigan 48109

(Received 29 February 1987; accepted for publication 19 May 1987)

Measurements and calculations have been carried out to determine the structure of electric potential and ion density in the near wake created by the flow of a high-Mach-number plasma past a conducting plate biased with respect to the undisturbed plasma. Results are obtained for a molecular nitrogen plasma with ambient electron densities N of the order of 10^5 cm^{-3}, ion temperatures of $\theta_i \simeq 0.025$ eV, electron temperatures of $\theta \sim 0.3$ eV, and plasma flow velocities of $V_0 \simeq 10^6$ cm/s, corresponding to $V_0/(\theta/M)^{1/2} \simeq 11$. For high-Mach-number flow past an unbiased object, the wake structure is very nearly that predicted for the expansion of an initially uniform plasma half-space into vacuum; in this case there is a sharply defined ion front moving under the influence of an electric field produced by charge separation between ions and electrons near the front. With bias potential ϕ_p such that $q\phi_p/\theta$ is in the range -1 to -10, a well-defined ion front still exists, but its motion is strongly affected by the imposed potential. This effect can be explained in terms of the impulse received by those ions passing through the sheath region near the plate edge. Two-dimensional simulations of the laboratory experiments were performed by using a multiple waterbag technique. The results for both zero and finite ion temperatures are almost noise-free and support the approximate analytical model. The calculated density for 10 θ negative bias on the plate is compared with the measured profile.

I. INTRODUCTION

A number of authors have reviewed the structure of the wake generated by relative motion between an object and a collisionless plasma.[1-5] These reviews have considered the wake structure extending from the near wake to the far wake for various ranges of body size R_0 relative to the ambient plasma Debye length λ_D and for various conditions of electrical potential on the body relative to the ambient plasma.

This study focuses on the structure of the ion front in the near wake behind a semi-infinite plate and, in particular, on the effect of plate potential on the structure of the ion front. The present analysis, which is relevant to the wake structure of a large body traversing the ionosphere, is motivated by the experiments on wakes performed in a large vacuum tank.[6] Figure 1 depicts the experimental situation. The measured results obtained by means of a differential ion-flux probe consist of ion-density profiles as a function of x at a given downstream position. The plate is biased to a potential ϕ_p relative to the tank wall, and ϕ_p may differ from the potential ϕ_a of the plasma in the neighborhood of the plate. The effect of ϕ_p (or $\phi_p - \phi_a$) on the motion and structure of the ion front in the wake behind the plate is determined.

The analysis, exploiting the approximate relationship between the problems of a mesosonic wake and the expansion of plasma into vacuum, considers first the effect of an applied electric field on the initial plasma expansion. Specific calculations of wake structure, including the effect of an applied potential and of ion temperature, are given and compared with experiment in Sec. IV.

II. EFFECT OF POTENTIAL ON EXPANSION INTO VACUUM

For zero bias the electric field at the ion front $x_F(z)$ is given approximately by[7]

$$\frac{qE}{M} = 2\sqrt{\frac{\theta}{M}}\frac{\alpha\omega}{1+\alpha\omega t}\left[1-\left(1-\frac{(2e)^{-1/2}}{\alpha}\right)\frac{1}{1+\alpha\omega t}\right], \quad t = z/V_0, \tag{1}$$

with the adjustable parameter α, $e = 2.718$, and ions travel with velocity V_0 in the positive Z direction. Here q and M are

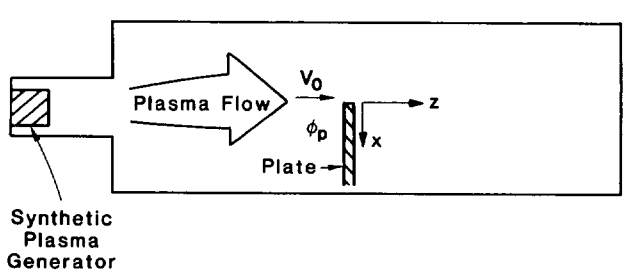

FIG. 1. Schematic illustration of experiment to measure ion density in wake behind a biased plate.

 0021-8979/87/192675-05$02.40

the ion charge and mass, respectively, θ the electron temperature, and $(\omega = Nq^2/\epsilon_0 M)^{1/2}$ the ion plasma frequency for ambient density N. The semiempirical formula (1) was constructed to reproduce, independent of α, certain theoretically known properties of expansion of a plasma half-space into vacuum, namely, the asymptotic dependence of the ion front on t for $\omega t \gg 1$,[8] and the value of E at $t = 0$, namely, $E_0 = (2N\theta/\epsilon_0 e)^{1/2}$.[9] The position and velocity of the front calculated from Eq. (1) are in good agreement with the measurements of Wright *et al.*[6]

Let us now consider how the expansion into vacuum is modified by an applied field E_i in the vacuum region. Initially, the ion density is N (uniform) for $x < 0$ and zero for $x > 0$. The potential is determined from

$$-\epsilon_0 \nabla^2 \phi = Nq[1 - \exp(q\phi/\theta)], \quad x < 0,$$
$$= Nq \exp(q\phi/\theta), \quad x > 0, \tag{2}$$

and satisfies the conditions $\phi \quad (x = -\infty) = 0$, $\phi(x = \infty) = -\infty$, $E \quad (x = -\infty) = 0$, and $E \ (x = \infty) = E_i$. The first integral of (2) over the plasma half-space from $x = -\infty$ to 0 yields

$$(\epsilon_0/2)\, E_0^2 = N\theta\, [\exp(q\phi_0/\theta) - 1 - q\phi_0/\theta\,], \tag{3}$$

where a subscript 0 denotes the value at the plasma-vacuum interface. Integration over the vacuum region yields

$$(\epsilon_0/2)(E_0^2 - E_i^2) = N\theta \exp(q\phi_0/\theta). \tag{4}$$

For $E_i = 0$, $\phi_0 = \phi_{00}$, and $E_0 = E_{00}$, where

$$q\phi_{00}/\theta = -1, \tag{5}$$

$$(\epsilon_0/2)E_{00}^2 = N\theta e^{-1}, \tag{6}$$

are the results obtained by Crow *et al.*[9] For $E_i \neq 0$,

$$(-\epsilon_0/2)E_i^2 = N\theta(1 + q\phi_0/\theta), \tag{7}$$

$$\tfrac{1}{2}E_0^2 = \tfrac{1}{2}E_i^2 + \tfrac{1}{2}E_{00}^2 e^{-\epsilon_0 E_i^2/2N\theta}. \tag{8}$$

The applied field is the dominant component of the initial field if $\epsilon_0 E_i^2/2N\theta > 1$. The applied field is, of course, a nebulous quantity; in particular, it is not unambiguously related to the value of the bias potential on an object over which a plasma is flowing. The order of magnitude, however, E_i should be comparable to that of the sheath electric field that deflects the streaming ions before they enter the near wake downstream from the object; $E_i \sim \phi_0/R$, where ϕ_0 is the potential on the object relative to that in the remote upstream plasma, and R is a length scale for potential variation within the sheath. Rather than attempting to further pursue the analogy between the plasma expansion and the wake problems, we turn now to consideration of the two-dimensional steady wake.

III. QUALITATIVE EFFECT OF POTENTIAL ON A TWO-DIMENSIONAL STEADY-STATE WAKE

The expansion of a semi-infinite plasma into vacuum corresponds only approximately to the wake problem. In particular, the free-expansion analog does not take into account the fixed potential on the wake-forming plate; nor does it clearly suggest how to account for variations in plate potential. A complete theory would be based on the steady-state solutions of the Poisson and ion trajectory equations in at least two dimensions.

A primary effect neglected in the free-expansion model is the transverse acceleration experienced by ions that pass from upstream ($z < 0$) through the sheath surrounding the tip of the plate before entering the wake region ($z > 0, x > 0$) (see Fig. 1). The sheath should extend in the upstream direction no more than a few λ_D, for $\phi_p \lesssim 10\,\theta$. In these circumstances the approximate effect of the sheath on fast ions ($\frac{1}{2}MV_0^2 \gg \phi_p$) can be described in terms of an impulsive change in transverse velocity V_x:

$$M\,\Delta V_x \simeq qE\,\Delta t \simeq (|q\phi_p|/R)\ (R/V_0), \tag{9}$$

where R is the range of the force, i.e.,

$$\Delta V_x/V_0 \simeq q\phi_p/MV_0^2. \tag{10}$$

For the following parameters, corresponding to conditions in Wright's experiments,[6]

$$\phi_p = -3 \text{ V},$$
$$\tfrac{1}{2}MV_0^2 = 18 \text{ V } (N_2^+),$$
$$\Delta V_x/V_0 \simeq \tfrac{1}{12}.$$

At a point $z = 22.4$ cm downstream, $\Delta x_{est} = (z/V_0)\Delta V_x \sim 2$ cm, where Δx_{est} is the estimated value.

The assumption that the effect of the finite plate potential on the wake is to deliver impulse to the ions means that the position x_F of the ion front will have shifted by an amount Δx relative to that for an unbiased plate. The shift in experimental values of x_F between $\phi_p = 0$ and $\phi_p = -3$ V is

$$\Delta x_{expt} = 0.65 \text{ cm},$$

where Δx_{expt} is the experimental value. Although of the right order of magnitude, the estimated Δx_{est} is 3 times Δx_{obs} (the observed value) even before taking account of the effect of potential in the downstream direction. In any case, the impulse approximation given leads to a displacement linear in applied potential, a conclusion not inconsistent with experimental results, at least for negative potentials.

For positive potentials the effect of potential appears to be smaller than for negative potentials, except for an abrupt change between $\phi = 0$ and $+1$ V. A smaller effect could be expected on the grounds that in the neighborhood of the plate the plasma will be only a few θ below ϕ_p for $\phi_p > 0$.

IV. TWO-DIMENSIONAL CALCULATIONS OF NEAR-WAKE STRUCTURE

The experiment was simulated numerically in two dimensions by using a finite-element computer code. The code solves the Poisson–Vlasov equations in steady state. Potentials, ion trajectories, and ion densities were calculated self-consistently on the finite-element mesh shown in Fig. 2. The boundary conditions were zero potential at the top (ambient plasma) and left (input) boundaries, specified (imposed bias) potential on the metal plate, zero normal component of electric field on the right (exit) boundary, and $E_\perp = 2\exp(\phi/\theta)$ on the lower (vacuum) boundary. For the finite-element potential solution the potential was assumed

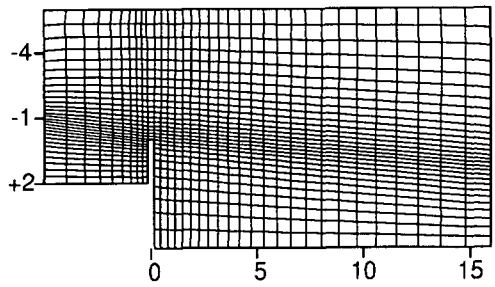

FIG. 2. Finite-element mesh used to calculate potentials and ion trajectories in the wake behind a biased plate. (Distances are in Debye lengths.)

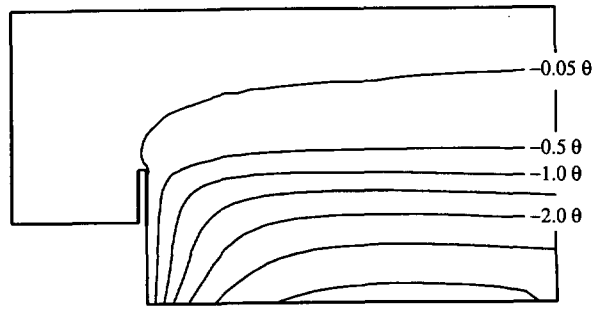

FIG. 4. Electrostatic potential contours for the zero-bias potential case at zero transverse ion temperature. Contour levels are at intervals of half the electron temperature. The same plot for finite ion temperature is indistinguishable from this one.

to vary bilinearly in each element. For calculating trajectories, however, a quadratic form was used to interpolate in the direction approximately normal to the ion front. This was necessary because the discontinuous electric fields obtained from linear interpolation caused bunching of ion trajectories, resulting in striations in the downstream ion density.

The ion density was calculated by using a variant of the "waterbag" method.[10,11] This method takes advantage of the fact that, if trajectories do not cross, the current contained between two trajectory paths (in two dimensions or in a "flux tube" in three dimensions) is constant. Denoting by u the dimension along the trajectories and by w the dimension normal to the trajectories, we have

$$I\,\Delta t = nv\,\Delta w\,\Delta t = n\,\Delta w\,\Delta u,$$

where n and v are the local ion density and velocity, respectively. It follows that the density ratio for quadrilaterals formed by adjacent time points on adjacent trajectories (Fig. 3) is the inverse ratio of their areas. Calculations were performed with initial (left boundary of grid) values of 0.1 and 0.2 Debye lengths for Δw and Δu, respectively, with constant time steps Δt. For the finite-temperature case the ions were divided into ten subspecies, each representing a different value of transverse velocity, and the resultant subspecies densities were added together. This technique for calculating ion densities resulted in very little numerical noise and no code diffusion, and proved far superior to particle-in-cell methods for cases such as this where a sharp ion-density boundary exists.

The electron density was assumed to satisfy the "barometric law"

$$n_e/N = \exp(q\phi/\theta)$$

for negative potentials and

$$n_e/N = 1 + q\phi/\theta$$

for positive potentials, where N and θ are the ambient plasma density (10^{-5} cm^{-3}) and electron temperature (0.27 eV), and ϕ is the local potential. Ion densities and potentials were iterated until neither changed more than 1%.

Figure 4 shows the electrostatic potentials calculated for the zero-temperature, zero-bias case. There are no electric fields seen upstream of the plate. Downstream, beyond a transition region of about 1 Debye length, the equipotential lines are nearly parallel to the ion flow direction, and equivalence to the one-dimensional time-dependent problem[9] is nearly exact. (Note that the influence of the plate extends several Debye lengths into the vacuum region.) The electrostatic potential for the case of the plate biased to $-10\,\theta$ is shown in Fig. 5. In this case the ions see very strong downward fields as they pass over the plate, providing the impulse described in Eq. (10). Moreover, the influence of the plate potential is strongly felt by the ions for about 10 Debye lengths downstream, providing additional downward force on the ion front.

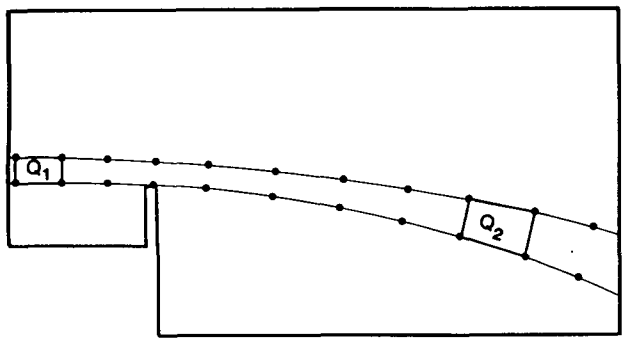

FIG. 3. Schematic of method for determining ion densities. Quadrilaterals are drawn between adjacent time points of adjacent trajectories. The density ratio is the inverse of the area ratio.

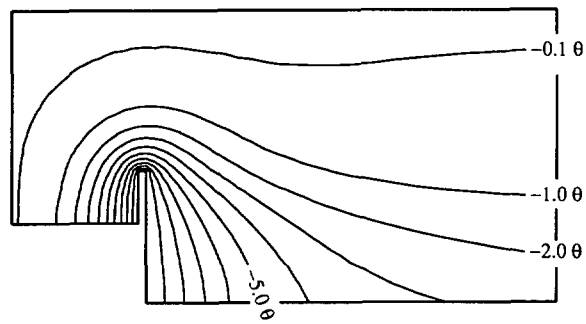

FIG. 5. Electrostatic potentials contours for bias potential of $-10\,\theta$ at finite (300-K) transverse ion temperature. Contour levels are at intervals of the electron temperature. The same plot for zero ion temperature is indistinguishable from this one.

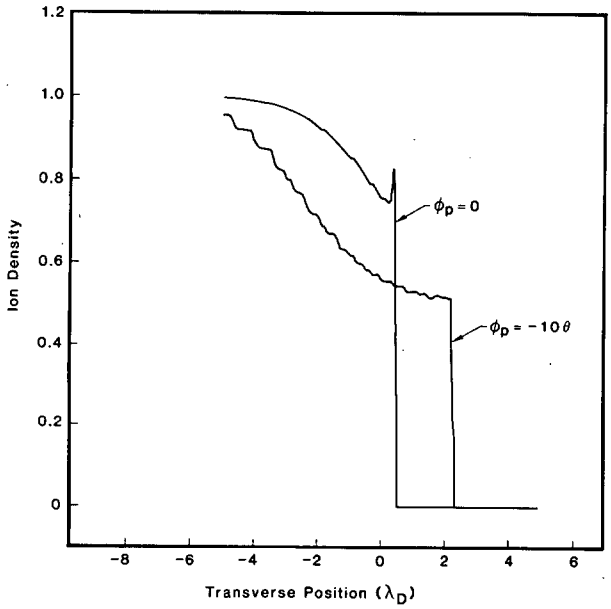

FIG. 6. Ion-density profiles for zero ion temperature calculated 15 Debye lengths downstream of the plate. The two curves are for plate bias potentials of zero (showing a peak and sharp drop at -0.5 Debye lengths) and $-10\,\theta$ (showing a sharp drop at -2.3 Debye lengths).

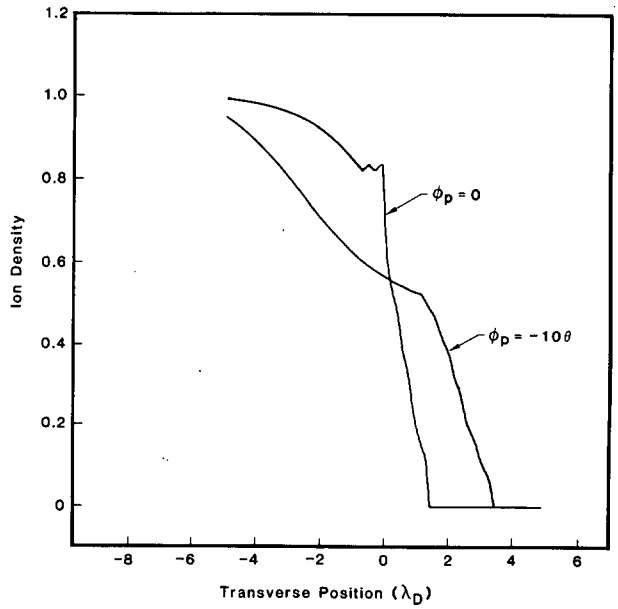

FIG. 7. Ion-density profiles for finite (300-K) ion temperature calculated 15 Debye lengths downstream of the plate. The two curves are for plate bias potentials of zero (showing a broadened front from $+0.1$ to 1.3 Debye lengths) and $-10\,\theta$ (showing a broadened front from -1 to -3 Debye lengths).

Ion-density profiles calculated 15 Debye lengths downstream of the plate are shown in Fig. 6 for cold ions and in Fig. 7 for a transverse ion temperature θ_i of $0.096\,\theta$ (300 K). The two curves in each figure are for plate potentials of zero and $-10\,\theta$. The increase in front motion (about 1.8 Debye lengths) corresponds closely with the 2 cm obtained from Eq. (10). The finite-temperature profiles are monotonic and considerably broader than the cold-ion profiles. The angular spread of the ion front is a few times $(2\theta_i/MV_0^2)$, as expected. The only nonmonotonic behavior is for cold ions with

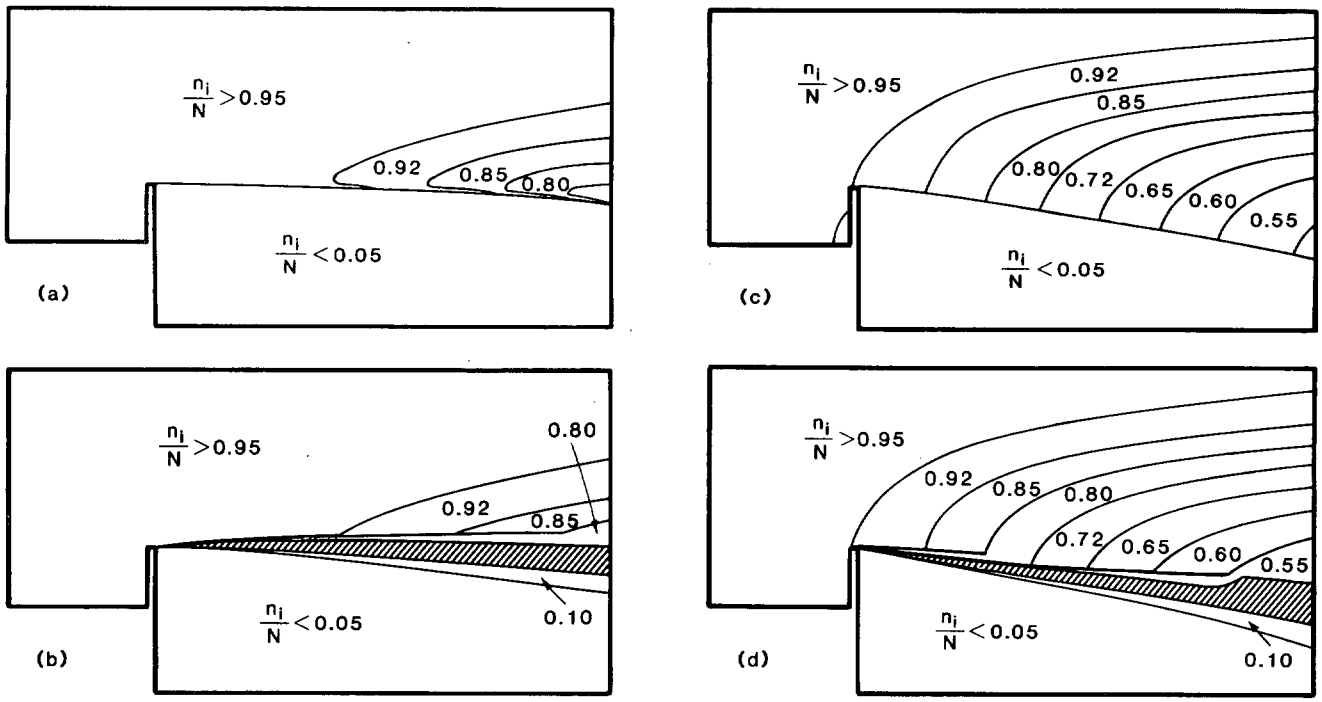

FIG. 8. Ion densities for (a) zero temperature, zero bias; (b) finite (300-K) temperature, zero bias; (c) zero temperature, $-10\,\theta$ bias; and (d) finite (300-K) temperature, $-10\,\theta$ bias. The spacing between contour levels is approximately 0.06, with several contour lines on the discontinuity [(a) and (c)] or in the shaded region [(b) and (d)].

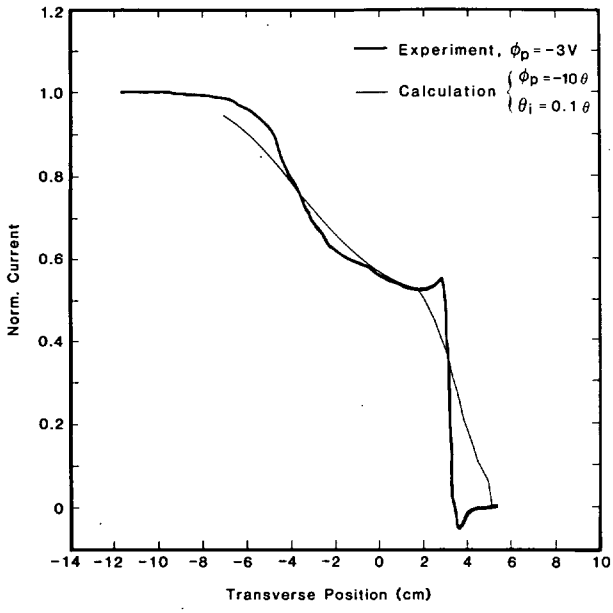

FIG. 9. Measured ion-density profile for -3-V bias, together with the calculated curve for 300-K ion temperature and $-10\,\theta$ bias.

zero potential on the plate. Figures 8(a)–8(d) show the calculated densities throughout the region for the four cases.

The calculated finite-temperature ion density is compared with the laboratory measurement in Fig. 9. The general front amplitude and motion agrees well with experiment. However, the calculation has a broader front, while the experiment evidences an overshoot and undershoot.

V. DISCUSSION

The calculated and experimental results show that wake closure is well described by the acceleration of ions in the plasma steady-state electric field. However, the electrostatic influence of the object creating the wake leads to significant differences between wake closure and the expansion of a plasma into vacuum.

For zero ion temperature and zero bias on the plate, the calculated front position ($0.50\lambda_D$) is less than theoretically predicted ($0.72\lambda_D$). This is due to the reduction of the transverse electric field at the front by the influence of the conducting plate for several λ_D downstream. The experimentally measured front position ($1.5\lambda_D$) is appreciably greater than predicted.

The application of $-10\,\theta$ bias to the plate dramatically changes the electrostatic potential structure. The shift in front position predicted by the crude "impulse" theory ($1.1\lambda_D$) is in qualitative agreement with calculation ($1.8\lambda_D$). The experimental shift ($0.5\lambda_D$) is smaller, but the resultant front positions ($2\lambda_D$, experiment; $2.3\lambda_D$, calculation) agree well. Experiment and calculation also show excellent agreement as to the magnitude of density change at the ion front.

The calculations produce the expected thermal spread in the front. The experimental thermal spread is far less, suggesting that the transverse ion temperature is well below 300 K. (Had we shown the zero-temperature calculation in Fig. 9, apparent agreement would have been near perfect.) However, an ion temperature of 300 K produces no observable change (relative to zero-temperature ions) in the electrostatic potential. We believe that the reason for lack of thermal spread in the experimental wake front is that the ions originate from a small source, so that they are already "velocity selected" when they enter the wake region.

Expansion of plasma into vacuum is a good approximate model for filling in a plasma wake. However, multidimensional effects due to the influence of the body creating the wake on the electrostatic potential structure cause noticeable departures from this model when the body is at plasma potential and substantial departures when the body departs from plasma potential.

ACKNOWLEDGMENT

This work supported by Air Force Geophysics Laboratory, Hanscom Air Force Base, MA, under Contract No. F19628-86-C-0056.

[1] Y. L. Al'pert, A. V. Gurevich, and L. P. Pitzaevskii, *Space Physics with Artificial Satellites* (Plenum, New York, 1965).
[2] V. C. Liu, Space Sci. Rev. **9**, 423 (1969).
[3] A. V. Gurevich, L. P. Pitaevskii, and V. V. Smirnova, Space Sci. Rev. **9**, 805 (1969).
[4] V. C. Liu, Prog. Aerospace Sci. **16**, 273 (1975).
[5] N. H. Stone, "The Aerodynamics of Bodies in a Rarefied Ionized Gas with Applications to Spacecraft Environmental Dynamics," NASA Technical Paper No. 1933, 1981.
[6] K. H. Wright, Jr., N. H. Stone, and U. Samir, J. Plasma Phys. **33**, 71 (1985).
[7] I. Katz, D. E. Parks, and K. H. Wright, Jr., IEEE Trans. Nucl. Sci. **NS-32**, 4092 (1985).
[8] A. V. Gurevich and A. P. Mashcherkin, Sov. Phys.-JETP **53**, 937 (1981).
[9] J. E. Crow, P. J. Auer, and J. E. Allen, J. Plasma Phys. **14**, 65 (1975).
[10] H. L. Berk, C. E. Nielsen, and K. V. Roberts, Phys. Fluids **13**, 980 (1970).
[11] A. C. Calder and J. G. Laframboise, J. Comput. Phys. **65**, 18 (1986).